Hindawi Publishing Corporation
Advances in Tribology
Volume 2013, Article ID 213914, 8 pages
http://dx.doi.org/10.1155/2013/213914

Research Article

MOORA-Based Tribological Studies on Red Mud Reinforced Aluminum Metal Matrix Composites

S. Rajesh,[1] S. Rajakarunakaran,[1] R. Suthakarapandian,[2] and P. Pitchipoo[3]

[1] *Department of Mechanical Engineering, Kalasalingam University, Anand Nagar, Krishnankoil 626126, India*
[2] *Nadar Saraswathi College of Engineering and Technology, Theni 625 531, India*
[3] *Department of Mechanical Engineering, P.S.R. Engineering College, Sevalpatti, Sivakasi 626 140, India*

Correspondence should be addressed to S. Rajesh; prinirajaki@yahoo.co.in

Received 25 May 2013; Accepted 5 September 2013

Academic Editor: Patrick De Baets

This paper presents the findings of an experimental investigation on the effects of applied load, sliding velocity, wt.% of reinforcement and hardness of the counterface material in dry sliding wear studies performed on red mud-based aluminum metal matrix composites (MMC). The specific wear rate and the coefficient of friction are considered as the output quality characteristics. Taguchi-based L_9 orthogonal array has been used to accomplish the objective of the experimental study. Analysis of variance (ANOVA) is employed to find the optimal setting and the effect of each parameter on the output performance characteristics. It has been observed that optimal factor setting for each output performance is different. In order to minimize the two responses simultaneously, multiobjective optimization based on ratio analysis (MOORA) is adopted. MOORA revealed that the optimal combination of the dry sliding wear parameters for the multiperformance characteristics of the red mud based aluminium is the set normal load at 20 N, sliding velocity 3 m/s, % of reinforcement 20%, and counterface hardness of the material 58 HRC.

1. Introduction

The metal matrix composites exhibit the significant increase in mechanical strength, wear resistance and damping properties when compared to matrix alloy [1, 2]. In many engineering applications the use of aluminium alloy is inevitable because of its superior mechanical, thermal property and it also possess low wear resistance property [3]. To increase the wear resistance of the aluminium, and its alloy is reinforced with different reinforcements, namely, short fibre, whiskers, and particulates [4]. Among the different reinforcement particulates reinforcement is gaining more attention because of its excellent isotropic property during the fabrication of composite [5].

Huda et al. [6] reported that selection of particular fabrication process depends on the type of the matrix and the reinforcement materials used to form the MMC. Particulates reinforcement can easily synthesise with matrix material using stir casting process. Sannino and Rack [7] reported that the particulates composites are good for industrial applications where performance along with cost is important. The effect of sliding velocity on the frictional and wear behaviour of aluminium MMC sliding against ferrous counterbody has been studied by a number of researchers. Unlu [8] conducted the experiments to investigate the effect of Al_2O_3-SiC reinforcement in aluminium metal matrix fabricated by casting and powder metallurgy method. The experiments results reveal that the tribological and the hardness property of the composites significantly improved by the use of reinforcement. Tang et al. [9] fabricated Al-B_4C composite to study the effect of dry sliding wear parameters, and it is found that the increasing wt.% of the reinforcement reduces the wear rate of the composites. Liu et al. [10] investigated the friction and wear property of short carbon reinforced aluminium matrix composites. The effect of fibre volume fraction, load applied, rotating speed and wear mechanics were discussed. It is found that the increasing wt.% of reinforcement decreases the wear rate and the increasing in applied load increases the wear rate. Rohatgi et al. [11] studied the dry sliding wear behaviour of Al 206 aluminium alloy containing silica sand reinforcement using three pins on disk rib meter against SAE 1045 steel.

The result revealed that the addition of silica sand reduces the coefficient of friction of the composites. Iwai et al. [12] adopted powder metallurgy method to fabricate SiC whisker reinforced 2024 Al composites for varying wt.% of reinforcements (0–16%). Based on the dry sliding wear parameter result, it is observed that the increase in wt.% of reinforcement decreases the wear rate.

Sahin and Ozdin [13] developed mathematical model for the abrasive wear behaviour of the SiCp reinforced aluminium metal matrix composites. From the experimentation it was found that the wear rate of the composites increases while increasing the applied load and abrasive size. Response surface method is used to evaluate dry sliding wear behavior of AA7075 aluminium-SiC composites produced by powder metallurgy. From their study, it is found that the sliding speed and particle size are directly proportional to wear rate whereas volume fraction is inversely proportional to wear rate [4]. It is found that the introduction of SiC particle reinforcement in the matrix alloy exerted the greatest effect on abrasive wear, followed by the applied load. The sliding distance is found to have much lower effect [13]. Many researchers have been using Taguchi method to identify the effect of parameters on dry sliding wear behavior of the composites. There has been experimental investigation using Taguchi and ANOVA to identify the significant factors, while testing with Al 2219 SiC and Al 2219 SiC-graphite material shows that the sliding distance, sliding speed, and load are having significant effect on wear [14]. Dharmalingam et al. [15] employed Grey Taguchi analysis (GRA) to identify the optimal combination of dry sliding wear parameter. The wear rate and coefficient of friction of the hybrid metal matrix composite (Al + SiC + MoS) are highly affected by wt.% of reinforcement, sliding speed, and applied load.

A few attempts have been made to fabricate MMC to increase the wear resistance characteristics using low cost reinforcement like bauxite, corundum, granites, and sillimanite [16]. The ever-increasing demand for low cost reinforcement stimulated the interest towards the utilization of red mud. Red mud is the byproduct arising from caustic bleaching of bauxite during production of alumina [17]. About 1-2 tons of red mud residues are produced for each ton of alumina and millions of tons of red mud have been accumulated with most of them being stored or released to sea. Storing of red mud in wetland possesses high alkalinity leading to soil alkalization and water pollution, and storing in dry land causes dust galore and pollute the atmosphere.

So, in this work an attempt is made to use red mud as reinforcement material and aluminium as matrix material. The present investigation has been carried out to optimize the wear and the coefficient of friction of the red mud reinforced aluminum metal matrix composite fabricated through the stir casting process.

2. Experimental Procedure

2.1. Materials. LM 25 aluminum alloy and red mud were used as matrix and reinforcement material. LM 25 aluminum alloy finds application in the electrical sliding contacts, cylinder blocks, cylinder heads, brakes, and other engine body castings. Reinforcement materials are added to the LM 25 alloy to enhance the strength of the part being manufactured. Tables 1 and 2 show the chemical composition of aluminum alloy and red mud material.

Table 1: Chemical composition of aluminum alloy.

Element	Cu	Mg	Mn	Fe	Ni	Zn	Al
wt.%	7.15	0.49	0.11	0.47	0.002	0.07	Rest

Table 2: Chemical composition of red mud.

Element	Fe_2O_3	Al_2O_3	TiO_2	SiO_2	Na_2O	CaO	V_2O_5	Others
wt.%	53.8	14.3	3.9	8.34	4.3	2.5	0.38	Balance

The red mud used for the present investigation is collected from the National Aluminum Company Limited (NALCO) Damanjodi, Odisha, India. The size of the red mud particles used for the study is in a range of 125–150 μm.

LM 25 aluminum alloy was cut into pieces from the ingot and pickled in 10% sodium hydroxide solution at 95–100°C for 10 minutes. The sinut formed was removed by immersing in a mixture which equally contains nitric acid and water, before washing in methanol. Immediately after drying up in the air, the weighed quantity of pickled aluminum was melted in a crucible. The required quantity of red mud (15, 20 and 25%) was taken in the powder containers. The red mud was preheated in the electrical furnace up to 800°C and maintained the temperature before mixing with aluminum melt.

The weighed quantity of pickled aluminum was melted to desired superheating temperature of 750 ± 10°C in graphite using crucible electrical resistance furnace with temperature controlling device. After melting was over, the required quantity of red mud particulates was preheated to around 800 ± 10°C to add to the molten metal and stirred continuously by using mechanical stirrer. The stirring time was maintained between 120 s at an impeller speed of 600 rpm. To enhance the wettability of red mud particles, small quantities of magnesium were added to the melt during stirring. The melt with the reinforced particulates was poured to prepare composite specimen. The prepared composite was subjected to machining to produce a size of Φ 10 and 30 mm length to carry out the dry sliding wear experiments.

2.2. Characterization of Composites. Optical microscope was used to study the distribution of red mud reinforcement in aluminum matrix. Figures 1(a) and 1(b) show the SEM and EDX of 20% red mud reinforced aluminum metal matrix composites. From Figures 1(a) and 1(b), it is understood that the red mud is uniformly distributed in the aluminum matrix. From EDX it is understood that the composite contains aluminum, silica, and ferric compounds. Specimen was metallographically polished and etched prior to the microstructural characterization. Density of the fabricated composite was determined by Archimedes' principle. Hardness of the composites was evaluated using Brinell hardness number.

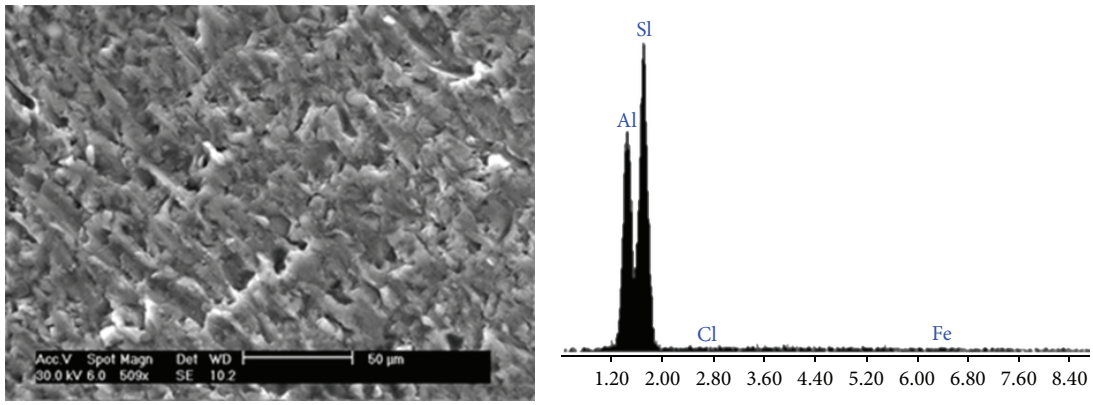

(a) (b)

Figure 1: SEM micrograph and EDX 20 wt.% red mud casted composite.

Table 3: Properties of the 20% red mud reinforced composites.

Sl. Number	Description	Value and units
1	Density	2.62 g/cm^3
2	Modulus of elasticity	42.8 GPa
3	Hardness	55.6 VHN
4	Impact strength	8.74 kg m/cm^2

Table 4: Properties of the counterface material.

Sl. Number	Description	Value and units
1	EN 32 steed hardness	58 and 60 HRC
2	Density	8.03 g/cm^3
3	Tensile strength	386 MPa
4	Yield strength	284.4 MPa

Table 3 shows the physical and mechanical properties of the composites.

2.3. Wear Test. Pin-on-disc wear testing apparatus (ASTM G99-95 (2006) standard) was used for performing dry sliding wear test for evaluating wear characteristics of the fabricated composites. Before conducting the test, the testing pin and the disc surfaces were polished with emery papers, and surface roughness (R_a) value was maintained in the range of 0.8 to 1.2 μm. Three different counter face materials with different hardness were used to conduct the experiment. Table 4 shows the properties of the counterface material. The surface roughness of the counter face was maintained at 3.8 to 4.0 μm. Polished samples were cleaned with acetone prior to wear testing. Prior to and after the wear tests, samples were weighed to measure the mass loss. The conformal type contact is used to study the specific wear rate and coefficient of friction of the composites. The contact pressure is maintained at 0.55 MPa.

The dry sliding wear performance of the composites was studied as function of load, sliding velocity, wt.% of reinforcements, and counter face hardness of the material.

Table 5: Dry sliding wear parameters and levels.

Dry sliding wear parameter	Level 1	Level 2	Level 3
Applied load (A) in N	10	20	30
Sliding velocity (B) in m/s	2	3	4
wt.% of reinforcement (C)	15	20	25
Hardness of the counterface (D) in HRC	58	60	62

The dry sliding wear tests were carried out at controlled temperature with sliding velocity of 2, 3, and 4 m/s. The applied normal load varied from 10 to 30 N with a step of 10 N. Constants sliding distance was maintained at 3000 m for all the tests. The coefficient of friction (cof) was computed from the applied load and the tangential load which was obtained from the strain gauges. Specific wear rate of the composites was calculated from the ratio of volume loss to applied load and sliding distance. The worn surfaces at the end of the tests were examined and analyzed using SEM.

2.4. Taguchi Experimental Design. Taguchi design of experiment is a powerful analyzing tool for modelling and analysis the effect of control factors on output response. In design of experiment, the most important stage is selection of control factors. The specific wear rate and coefficient of friction characteristics of the dry sliding wear are affected by applied load (A), sliding velocity (B), wt.% of reinforcement (C), and hardness of the counter face material (D). The dry sliding wear conditions under which tests were carried out are given in Table 5.

Four process parameters at three levels led to the total of 9 dry sliding wear tests. The constant sliding distance was maintained at 3000 m for all the experiments. In this study, the standard L_9 orthogonal array was chosen which had 13 rows corresponding to the number of parameters combination with 8 degrees of freedom.

The objective of the experimentation is to reduce the specific wear rate and coefficient of friction as small as possible. In Taguchi method, signal-to-noise (S/N) ratio is used to represent a performance characteristic and the largest value

Table 6: Experimental runs and results.

Sl. Number	Applied load in N	Sliding velocity in m/s	wt.% of reinforcement	Hardness in HRC	Specific wear rate $\times 10^{-3}$ mm^3/N m	Coefficient of friction (μ)
1	10	2	15	58	0.13	0.48
2	10	3	20	60	0.08	0.57
3	10	4	25	62	0.01	0.44
4	20	2	20	62	0.15	0.62
5	20	3	25	58	0.16	0.61
6	20	4	15	60	0.08	0.59
7	30	2	25	60	0.11	0.64
8	30	3	15	62	0.15	0.56
9	30	4	20	58	0.11	0.62

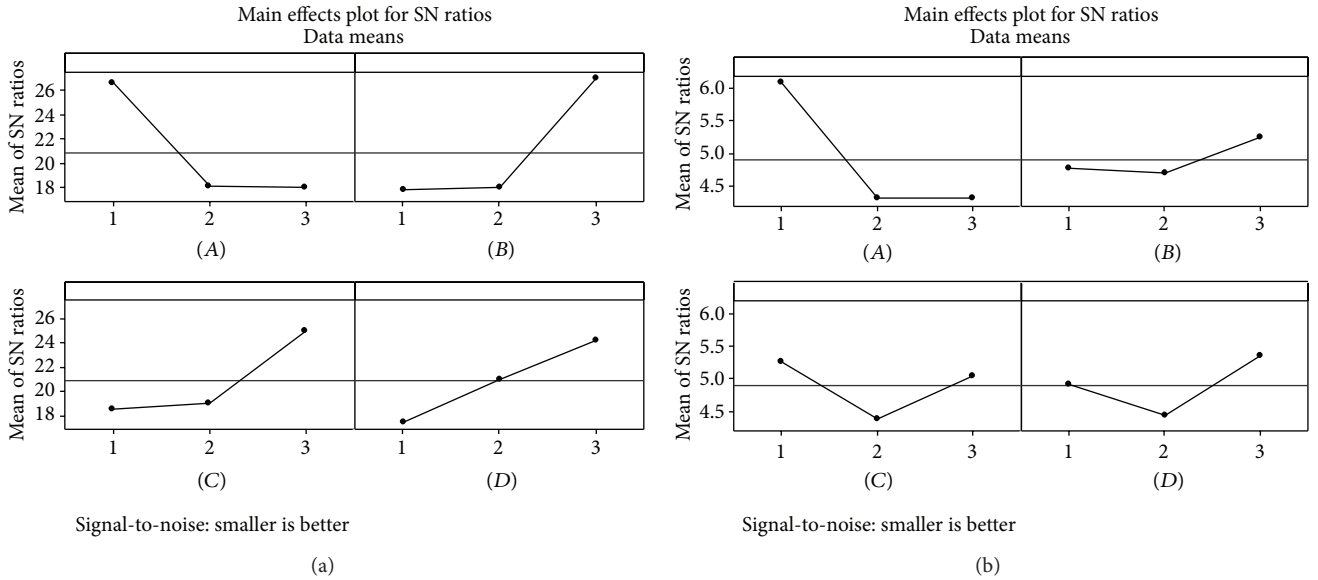

Figure 2: Main effect plot. (a) Specific wear. (b) Coefficient of friction.

of S/N ratio is required. There are three types of S/N ratio—the lower-the-better, the higher-the-better, and the nominal-the-better. In this work, the lower-the-better characteristic is required for all output responses hence lower-the-better characteristic can be expressed as;

$$\eta_{ij} = -10 \log \left(\frac{1}{n} \sum_{j=1}^{n} y_{ij}^2 \right), \quad (1)$$

where, η_{ij} is the jth S/N ratio of the ith experiment, y_{ij} is the ith experiment at the jth test, and n is the total number of the tests.

Table 6 shows the orthogonal array and results obtained during the experimentation. Equation (1) is used to calculate the S/N ratio for the output performance characteristics using Minitab software version 16. Figures 2(a) and 2(b) show the S/N ratio main effect plot for the output performance characteristics. From Figures 2(a) and 2(b) it was understood that the optimal parameter combination for specific wear rate was A_1, B_3, C_3, D_3 and for coefficient of friction was A_1, B_3, C_1, D_3. Table 7 shows the optimal condition for specific wear rate and coefficient friction. In this work less number data is utilized for optimization of dry sliding wear parameters; hence it is mandatory to conduct confirmation experiments. This confirmation experiment is used to verify the improvement in the quality characteristics. The confirmation experiment was carried out for two optimal factors setting, since the specific wear rate and coefficient of friction have different optimal combinations. To verify the accuracy

Table 7: Optimum factor level.

Factors	Specific wear rate	Coefficient of friction
A	1	1
B	3	3
C	3	1
D	3	3

Table 8: ANOVA for specific wear rate.

Factors	Levels S/N			DF	SS	V	F	P (%)
	1	2	3					
A	26.55	18.11	18.00	2	0.0049	0.0024	0.0024	22.33
B	17.79	17.96	26.91	2	0.0062	0.0031	0.0031	28.28
C	18.56	19.07	25.03	2	0.0070	0.0035	0.0035	31.79
D	17.47	21.02	24.17	2	0.0038	0.0019	0.0019	17.5
Total				8				

DF: degree of freedom, SS: sum of squares, V: variance, F: test, P: contribution.

Table 9: ANOVA for coefficient of friction.

Factors	Levels S/N			DF	SS	V	F	P (%)
	1	2	3					
A	6.079	4.310	4.305	2	0.024	0.012	0.0120	67.47
B	4.760	4.692	5.242	2	0.002	0.0009	0.0009	5.059
C	5.268	4.377	5.049	2	0.005	0.0025	0.0025	14.22
D	4.908	4.428	5.357	2	0.005	0.0023	0.0023	13.23
Total				8				

of the model values are predicted using (2) at optimum factor level setting and compared with experimental results:

$$\mu_{\text{predicated}} = \mu_m + \sum_{i=1}^{n} (\mu_0 + \mu_m), \tag{2}$$

where μ_m is the mean S/N ratio, μ_0 is the mean S/N ratio at optimum level, and n is the number of dry sliding wear parameters that affect the output characteristics.

The small error of 3.1, and 4.4% between the predicted and experimental value for specific wear rate and coefficient of friction, respectively, proves the stability of the resulting model.

The relative influence factor of the dry sliding parameter on the specific wear rate and the coefficient of friction is determined by ANOVA. Tables 8 and 9 show the results of ANOVA for the specific wear rate and the coefficient of friction. It is observed from Tables 8 and 9 that the effect of each parameter on output performance characteristics is varying. In case of specific wear rate, wt.% of reinforcement is the predominant factor followed by sliding speed, applied load, and hardness of the counter face material, whereas coefficient of friction is highly influenced by applied load than wt.% of reinforcement, hardness of the counter face material, and sliding speed. Taguchi-based model is capable of finding optimal factor level for single objective problems. But model is to be developed to minimize the variation in all the responses simultaneously at the common factor level settings. To achieve this, multiobjective optimization using MOORA method is employed.

2.5. MOORA Method (Multiobjective Optimization by Ratio Analysis). MOORA was introduced by Brauers and Zavadskas [18] and they themselves enhanced the method to solve multiobjective problem. Now it becomes a powerful tool in engineering domain [19]. This method has been applied in numerous studies to solve various complex decision-making problems in the engineering environment. This method starts with a matrix of responses of different alternatives to different objectives. MOORA refers to a ratio system in which each response of an alternative on an objective is compared to a denominator, which is the representative for all alternatives concerning that objective. For this denominator, the square root of the sum of squares of each alternative per objective is chosen [20],

$$Nx_{ij} = \frac{x_{ij}}{\sqrt{\sum_{j=1}^{m} x_{ij}^2}}, \tag{3}$$

where Nx_{ij} is a dimensionless number representing the normalized response of alternative j to objective i; these normalized responses of the alternatives to the objectives belong to the interval [0; 1]. For optimization, these responses are added in case of maximization and subtracted in case of minimization:

$$Ny_j = \sum_{i=1}^{i=g} Nx_{ij} - \sum_{i=g+1}^{i=n} Nx_{ij}. \tag{4}$$

With $i = 1, 2, \ldots, g$ for the objectives to be maximized, $i = g + 1, g + 2, \ldots, n$ for the objective to be minimized, Ny_j is a normalized assessment of alternative j with respect to all objectives. In this formula linearity concerns dimensionless measures in the interval $[0, 1]$. Finally ordinary ranking method is employed to rank the alternatives.

3. Result and Discussion

The experimental result of various performance characteristics is normalized and turned into nondimensional values using (3). Table 10 shows the values of Nx_{ij}, where Nx_{ij} numbers represent the normalized responses for all output

Table 10: Normalized ratio and MOORA ranking.

Sl. Number	Normalized S/N ratio	Subtracted value	Rank
1	17.72	−0.3212	6
2	21.93	−0.2765	8
3	40.00	−0.1426	9
4	16.47	−0.3896	2
5	15.91	−0.4004	1
6	21.93	−0.2829	7
7	19.17	−0.3393	5
8	16.02	−0.3846	3
9	18.78	−0.3402	4

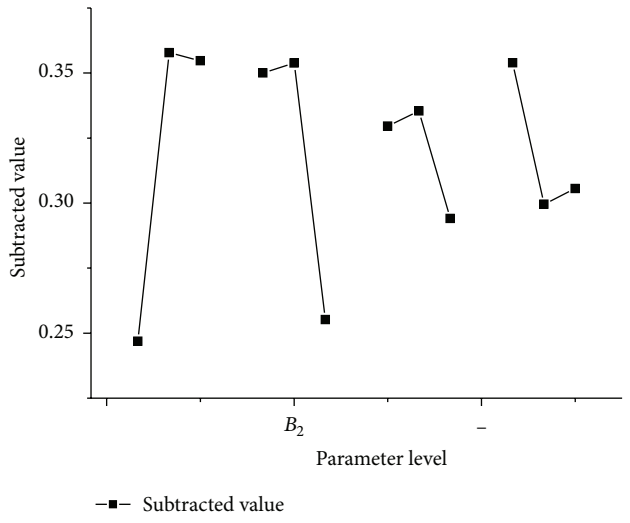

Figure 3: Graph for subtracted value.

response characteristics. The complex rationality between the output characteristics is calculated by using (4). In this work all the performance characteristics are the smaller-the-better; hence for optimization the output responses are subtracted and it is listed in Table 10. The simple ranking procedure is adopted to find the optimal dry sliding parameter combination. The result obtained according to the ranking represents the best parameter setting. Ny_i values which are used to find the optimal combinations of the parameter are A_2, B_2, C_2, and D_1.

3.1. Best Experimental Run. The mean of the subtracted value for each level of the dry sliding wear parameter can be calculated by averaging the subtracted value. For the applied load, the experiment numbers are 1–3 for level 1, experiment numbers 4–6 for level 2, and experiment numbers 7–9 for level 3. Similarly, it is calculated for the respective levels for applied load, sliding velocity, wt.% of reinforcement, and hardness of the counterface material. The larger the value of the subtracted values, that the better the multiresponse characteristics. Figure 3 shows the response graph is drawn with the various levels of the dry sliding wear parameter. Based on this study, one can select a combination of the levels that provide the largest average response. In Figure 3, the combination of A_2, B_2, C_2, and D_1 shows the largest value of the subtracted value for the factors A, B, C, and D, respectively. Therefore, A_2, B_2, C_2, and D_1 show with the applied load of 20 N, sliding velocity of 3 m/s, and 20 wt.% reinforcement, and the hardness of the counter face material of 58 HRC is the optimal parameter combination of the dry sliding wear parameter of red mud-based aluminum metal matrix composites.

Table 11: Confirmation experiment.

Response	Initial parameter setting	Optimal parameter setting	Improvement in %
Setting level	$A_1\ B_3\ C_3\ D_3$	$A_2\ B_2\ C_2\ D_1$	—
Specific wear rate	10×10^{-5}	9.58×10^{-5}	4.2
Coefficient of friction	0.44	0.41756	5.1

Once the optimal level of the dry sliding wear parameters is identified, the following step is to verify the improvement of the performance characteristics. Table 11 shows the results of the confirmation experiment conducted based on optimal setting. To compare the effectiveness of optimal parameter setting ($A_2\ B_2\ C_2\ D_1$) the test is conducted based on the initial factor level setting ($A_1\ B_1\ C_1\ D_1$). From Table 11 it is found that there is good improvement in the output performance while using optimal settings. If the optimal setting with the applied load of 10 kN, sliding velocity 3 m/s, 20 wt.% of reinforcement, and the hardness of the counter face material of 58 HRC is used, the specific wear rate decreases from 10×10^{-5} to 9.58×10^{-5}, and the coefficient of friction decreases from 0.440 to 0.41756. From Table 11, it is understood that the multiple performance characteristics in dry sliding wear operation is greatly improved.

3.2. Worn Surface Analysis at Optimal Condition. The optimized result can be correlated with the SEM micrographs of the worn surface of red mud reinforced metal matrix composites. In aluminum—20 wt.% of red mud reinforcement clearly shows fine grooves in the surface and plastic deformation at few places when applying 3 m/s sliding velocity and 58 HRC counter face hardness of the material as shown in Figure 4. Specific wear rate of the composites decreased due to the exposure of red mud particles at the worn surface. These projected particles carry the normal load between the contact interfaces. This automatically reduces the load on aluminum matrix. Hence, these harder particles protect the progressive wear of aluminum matrix to some extent. By way of load sharing, presence of harder reinforcement restricts the surface deformation of metal matrix. Due to this reason higher reduction in wear rate is realized with the increase of red mud weight fraction.

From Figure 5 it is perceived that the increase in applied load, counter face hardness of the material, and sliding speed increases the wear rate of the composites due to the formation of larger grooves in the worn surfaces.

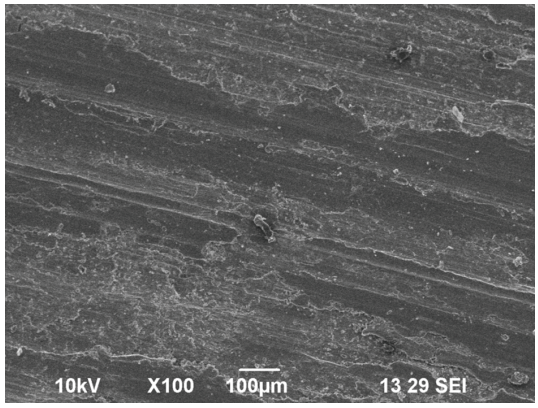

Figure 4: Worn surface of red mud reinforced aluminium matrix at optimal setting.

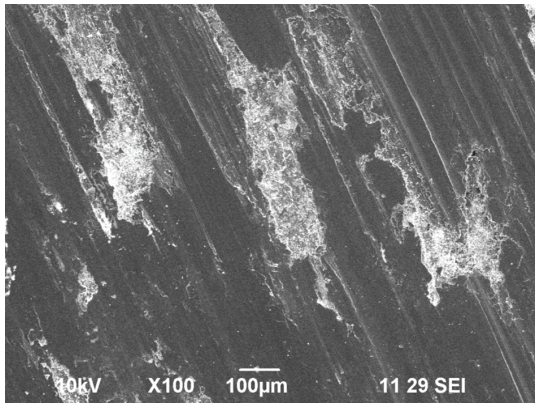

Figure 5: Worn surface of red mud reinforced aluminium matrix at 30 N and 4 m/s.

By comparing two results, it is also noticed that the addition 20 wt.% of reinforcement improves the formation of oxide layer which reduces the specific wear rate of the composite at 20 N load and at 3 m/s sliding velocity.

4. Conclusion

The use of the Taguchi method combined with the MOORA to optimize the dry sliding wear parameters of the red mud-based aluminum metal matrix composites by considering the multiple quality characteristics has been reported in this paper.

The following conclusions were made.

(i) For the lowest specific wear rate, 10 N applied load, 4 m/s sliding speed, 25 wt.% of reinforcement, and 62 HRC counterface hardness of the material were used.

(ii) For the lowest coefficient of friction, 10 N applied load, 4 m/s sliding speed, 15 wt.% of reinforcement, and 62 HRC counterface hardness of the material were used.

(iii) By analyzing the response graph of the average subtracted value, it is found that the largest value of the subtracted value of for the applied load is 20 N (A_2), sliding velocity of 3 m/s (B_2), % of reinforcement of 20% (C_2), and hardness of the counter face material of 58 HRC (D_1). This is the recommended level of the controllable parameters of the dry sliding wear parameter of the red mud based aluminum metal matrix composites, because the minimization of the specific wear rate and the coefficient of friction are simultaneously considered.

(iv) From the ANOVA, it is understood that the specific wear rate highly depends upon the wt.% of reinforcement (31.79%) followed by sliding velocity (28.28%), applied load (22.33%), and counter face hardness of the material (17.58%).

(v) It is also observed from the ANOVA table that the coefficient of friction of the composite material is highly affected by applied load (67.17%), % of reinforcement (5.05%), counter face hardness of the material (14.22%), and sliding velocity (13.23%).

(vi) Through the MOORA method, the reduction in the specific wear rate and the coefficient of friction of dry sliding wear parameter of red mud based aluminum metal matrix composites was observed when compared to the $A_1\ B_1\ C_1\ D_1$ to the optimized condition $A_2\ B_2\ C_2\ D_1$.

(vii) From this study it is also concluded that the wear resistance of the dry sliding wear parameter of the red mud based aluminum metal matrix composites has been enhanced greatly through MOORA method.

References

[1] R. L. Deuis, C. Subramanian, and J. M. Yellup, "Abrasive wear of aluminium composites—a review," *Wear*, vol. 201, no. 1-2, pp. 132–144, 1996.

[2] A. Alahelisten, F. Bergman, M. Olsson, and S. Hogmark, "On the wear of aluminium and magnesium metal matrix composites," *Wear*, vol. 165, no. 2, pp. 221–226, 1993.

[3] K. R. Brown, M. S. Venice, and R. A. Woods, "The increasing use of aluminium in automotive applications," *Journal of Materials*, vol. 47, pp. 20–23, 1995.

[4] S. Kumar and V. Balasubramanian, "Developing a mathematical model to evaluate wear rate of AA7075/SiCp powder metallurgy composites," *Wear*, vol. 264, no. 11-12, pp. 1026–1034, 2008.

[5] M. Rahimian, N. Parvin, and N. Ehsani, "The effect of production parameters on microstructure and wear resistance of powder metallurgy Al-Al_2O_3 composite," *Materials and Design*, vol. 32, no. 2, pp. 1031–1038, 2011.

[6] D. Huda, M. Baradie, and M. S. J. Hashoni, "Compaction behaviour of metal matrix composite," *Emerging Metals*, vol. 86, pp. 85–92, 1993.

[7] A. P. Sannino and H. J. Rack, "Dry sliding wear of discontinuously reinforced aluminum composites: review and discussion," *Wear*, vol. 189, no. 1-2, pp. 1–19, 1995.

[8] B. S. Unlu, "Investigation of tribological and mechanical properties Al_2O_3-SiC reinforced Al composites manufactured by

casting or P/M method," *Materials and Design*, vol. 29, no. 10, pp. 2002–2008, 2008.

[9] F. Tang, X. Wu, S. Ge et al., "Dry sliding friction and wear properties of B_4C particulate-reinforced Al-5083 matrix composites," *Wear*, vol. 264, no. 7-8, pp. 555–561, 2008.

[10] L. Liu, W. Li, Y. Tang, B. Shen, and W. Hu, "Friction and wear properties of short carbon fiber reinforced aluminum matrix composites," *Wear*, vol. 266, no. 7-8, pp. 733–738, 2009.

[11] P. K. Rohatgi, B. F. Schultz, A. Daoud, and W. W. Zhang, "Tribological performance of A206 aluminum alloy containing silica sand particles," *Tribology International*, vol. 43, no. 1-2, pp. 455–466, 2010.

[12] Y. Iwai, H. Yoneda, and T. Honda, "Sliding wear behavior of SiC whisker-reinforced aluminum composite," *Wear*, vol. 181–183, no. 2, pp. 594–602, 1995.

[13] Y. Sahin and K. Ozdin, "A model for the abrasive wear behaviour of aluminium based composites," *Materials and Design*, vol. 29, no. 3, pp. 728–733, 2008.

[14] S. Basavarajappa, G. Chandramohan, and J. Paulo Davim, "Application of Taguchi techniques to study dry sliding wear behaviour of metal matrix composites," *Materials and Design*, vol. 28, no. 4, pp. 1393–1398, 2007.

[15] S. Dharmalingam, R. Subramanian, K. Somasundara Vinoth, and B. Anandavel, "Optimization of tribological properties in aluminum hybrid metal matrix composites using gray-taguchi method," *Journal of Materials Engineering and Performance*, vol. 20, no. 8, pp. 1457–1466, 2011.

[16] M. Singh, B. K. Prasad, D. P. Mondal, and A. K. Jha, "Dry sliding wear behaviour of an aluminium alloy-granite particle composite," *Tribology International*, vol. 34, no. 8, pp. 557–567, 2001.

[17] Y. Zhang, A. Zhang, Z. Zhen, F. Lv, P. K. Chu, and J. Ji, "Red mud/polypropylene composite with mechanical and thermal properties," *Journal of Composite Materials*, vol. 45, no. 26, pp. 2811–2816, 2011.

[18] W. K. M. Brauers and E. K. Zavadskas, "The MOORA method and its application to privatization in a transition economy," *Control and Cybernetics*, vol. 35, no. 2, pp. 445–469, 2006.

[19] W. K. M. Brauers and E. K. Zavadskas, "Project management by multimoora as an instrument for transition economies," *Technological and Economic Development of Economy*, vol. 16, no. 1, pp. 5–24, 2010.

[20] V. S. Gadakh, "Application of MOORA method for parametric optimization of milling process," *International Journal of Applied Engineering Research*, vol. 1, pp. 743–757, 2011.